The Evolving Metropolis
2019 IABSE Congress New York City

IABSE 90 YEARS

Super-long span bridge aerodynamics: on-going results of the TG3.1 benchmark test – Step 1.2

Giorgio DIANA
Chair of Task Group 3.1
Politecnico di Milano
Italy
giorgio.diana@polimi.it

Stoyan STOYANOFF
Vice-chair of Task Group 3.1
RWDI
Canada
Stoyan.Stoyanoff@rwdi.com

Andrew ALLSOP
ARUP
United-Kingdom
andrew.allsop@arup.com

Luca AMERIO
ARUP
United-Kingdom
luca.amerio@arup.com

Tommaso ARGENTINI
Politecnico di Milano
Italy
tommaso.argentini@polimi.it

Miguel CID MONTOYA
University of A Coruna
Spain
miguel.cid.montoya@udc.es

Santiago HERNÁNDEZ
University of A Coruna
Spain
santiago.hernandez@udc.es

José Ángel JURADO
University of A Coruna
Spain
jjurado@udc.es

Igor KAVRAKOV
Bauhaus-University Weimar
Germany
igor.kavrakov@uni-weimar.de

Guy LAROSE
RWDI
Canada
Guy.Larose@rwdi.com

Allan LARSEN
COWI
City and Country
ALN@cowi.dk

Guido MORGENTHAL
Bauhaus-University Weimar
Germany
guido.morgenthal@uni-weimar.de

Simone OMARINI
Politecnico di Milano
Italy
simone.omarini@polimi.it

Daniele ROCCHI
Politecnico di Milano
Italy
daniele.rocchi@polimi.it

Martin SVENDSEN
Ramboll
Denmark
MNNS@ramboll.dk

Contact: tommaso.argentini@polimi.it

1 Abstract

This paper is part of a series of publications aimed at the divulgation of the results of the 3-step benchmark proposed by the IABSE Task Group 3.1 to define reference results for the validation of the software that simulate the aeroelastic stability and the response to the turbulent wind of super-long span bridges. Step 1 is a numerical comparison of different numerical models both a sectional model (Step 1.1) and a full bridge (Step 1.2) are studied. Step 2 will be the comparison of predicted results and experimental tests in wind tunnel. Step 3 will be a comparison against full scale measurements.

The results of Step 1.1 related to the response of a sectional model were presented to the last IABSE Symposium in Nantes 2018. In this paper, the results of Step 1.2 related to the response long-span full bridge are presented in this paper both in terms of aeroelastic stability and buffeting response, comparing the results coming from several TG members.

Keywords: benchmark; aeroelasticity; flutter; buffeting; long-span bridge.

2 Introduction

The objective of the IABSE Task Group 3.1 (TG) is the definition of a standard procedure for validating the software programs for the solution of the bridge response to the incoming turbulent wind (see [1][2]).

For this purpose, a 3-step benchmark was proposed, and it was started in 2017. The Step 1 of the benchmark is a numerical comparison of different solution methods, with the same inputs: critical flutter speed and buffeting response of both a sectional model and a full bridge are studied. Step 2 will be the comparison of predicted results and wind tunnel experimental tests, and Step 3 will be of comparisons against full scale measurements.

Step 1 consists of two sub-steps. In Step 1.1 the numerical response of 2/3 degree-of-freedom (DOF) simple sectional model is considered. The results are discussed in [2]. In Step 1.2 a full bridge model and a multi-correlated wind field are considered.

In this paper, the main results of Step 1.2 will be presented, highlighting critical issues and the main differences arisen during the comparison of the results.

The results presented are intended to be a reference for the validation of software programs that solves for wind response of bridges. An extended and complete report with Step 1 results will be issued in the near future.

3 Benchmark: Step 1.2

3.1 Step 1.2 Cases

Step 1.2 was conceived to analyze two sub-cases with increasing complexity:

a) Step 1.2a studies the stability and the buffeting response of a real full bridge forced by a turbulent wind field, where the horizontal and vertical components of wind velocity change in time and space (along the bridge axis). The Storebælt bridge structure is considered, using a modal approach to compute the dynamic response. Experimental aerodynamic coefficients at 0-degree angle of attack are used to simplify the analysis, since for this case no static deflection is considered.

b) Step 1.2b introduces additional complexity with respect to 1.2a: both the static deflection of the bridge and the dependency of the experimental aerodynamic coefficients upon the angle of attack are considered.

In this paper, selected key results of Step 1.1a-b are presented.

3.2 Input for the analysis Step 1.2

3.2.1 Structural data

Modal parameters of the first 12 modes of the bridge (mass, frequency and damping ratio) are reported in Table 1. The modal shapes of the deck are available and not reported here for brevity.

Table 1. Modal parameters

#	Mode	Frequency [Hz]	Damping ξ [-]
1	horizontal 1	0.0521	0.3%
2	vertical 1	0.0839	0.3%
3	vertical 2	0.0998	0.3%
4	horizontal 2	0.1179	0.3%
5	vertical 3	0.1317	0.3%
6	vertical 4	0.1345	0.3%
7	vertical 5	0.1827	0.3%
8	horizontal 3	0.1866	0.3%
9	torsional 1	0.2784	0.3%
10	vertical 6	0.2815	0.3%
11	torsional 2	0.3833	0.3%
12	vertical 7	0.3975	0.3%

3.2.2 Incoming turbulent wind

The characteristics of the simulated wind (along wind component *u* and vertical component *w*) are reported in Table 2. From these characteristics ten time series of 10-min turbulent wind were generated using a spectral approach for time domain simulations (e.g. [4]). The employed wind generator was selected for convenience whereas the investigation of wind and wind field generation problem is beyond the scope of this study. The time

histories of the vertical component and of the horizontal component are provided to all the participants. Each time history is 10 minutes long with a sampling frequency of 20 Hz.

The space coherence between u or w at two different points P and Q is:

$$\Lambda_{ii} = \exp\left(-\frac{2\sqrt{(C_{iz}\Delta_x)^2+(C_{iz}\Delta z)^2}\, f}{\overline{U_P}+\overline{U_Q}}\right) \quad (1)$$

where $i = u$ or w, $C_{ux} = 10$, $C_{uz} = 10$, $C_{wx} = 6.50$, $C_{wz} = 3$, $\Delta z = z_P - z_Q$ and $\Delta x = x_P - x_Q$.

The wind is discretized through 90 sections. Figure 1 shows the full bridge in blue and the 90 wind sections with red lines. Each wind section is 30 m long (about 1 deck chord B=31 m).

Table 2. Incoming wind characteristics

Wind speeds	U = 15, 30, 45, 60, 75 m/s
Air density	$\rho = 1.22$ kg/m^3
Turbulence intensity	$I_u = \frac{\sigma_u}{U} = 0.10$; $I_w = \frac{\sigma_w}{U} = 0.05$
Integral length scale	${}^xL_u$ = 200 m; ${}^xL_w$ = 20 m
***u* and *w* spectra**	$\frac{f\cdot S_u(f)}{\sigma_u^2} = \frac{4\left(\frac{f\,{}^xL_u}{U}\right)}{\left[1+70.8\left(\frac{f\,{}^xL_u}{U}\right)^2\right]^{5/6}}$ $\frac{f\cdot S_w(f)}{\sigma_w^2} = \frac{4\left(\frac{f\,{}^xL_w}{U}\right)\left(1+755.2\left(\frac{f\,{}^xL_w}{U}\right)^2\right)}{\left[1+283.2\left(\frac{f\,{}^xL_w}{U}\right)^2\right]^{11/6}}$ $S_{uw}(f) = 0$

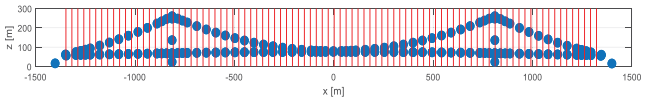

Figure 1. Full bridge and wind sections

3.2.3 Aerodynamic forces

Aerodynamic forces are applied only to the deck, to simplify the benchmark. The sign conventions for forces and displacements are shown in Figure 2 .

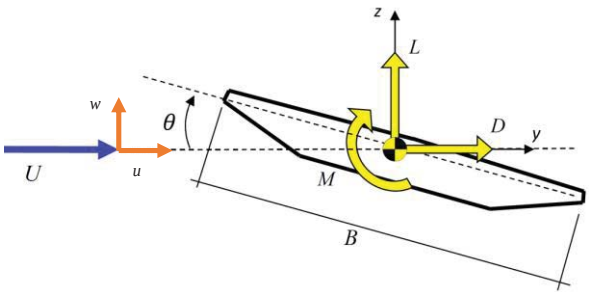

Figure 2. Sign conventions

The aerodynamic forces are modelled with the classical approach based on a linearized model of the fluid-structure interaction around a steady configuration of the bridge, which depends on the mean wind speed [2].

For Step 1.2a/b the experimental aerodynamic coefficients of the Yavuz Sultan Selim Bridge (Third Bosphorus Bridge, BB3) without windscreens are considered. The experimental tests have been performed on a 2 degree-of-freedom sectional in the Politecnico di Milano wind tunnel [3].

The steady aerodynamic drag, lift and moment coefficient per unit length as functions of the angle of attack α are defined as:

$$F_{ST} = \frac{1}{2}\rho U^2 B \begin{bmatrix} C_D(\alpha) \\ C_L(\alpha) \\ B\, C_M(\alpha) \end{bmatrix} \quad (2)$$

where B is the deck chord, U the mean wind velocity, and ρ the air density. C_D, C_L, C_M are respectively the drag, lift and moment static coefficients, reported in Figure 3.

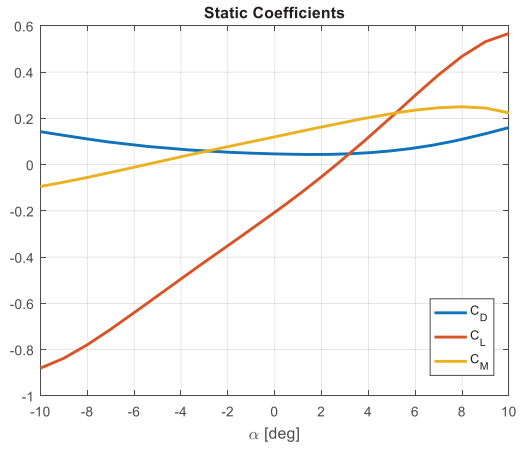

Figure 3. Static coefficients

The aeroelastic forces (self-excited forces F_{se}) per unit length are defined through the flutter

derivatives reported below in the Polimi formulation:

$$D_{se} = \frac{1}{2}\rho U^2 B \begin{pmatrix} -p_1^* \frac{\dot{z}}{U} - p_2^* \frac{B\dot{\theta}}{U} + p_3^* \theta + \dots \\ \frac{2\pi^3}{V^{*2}} p_4^* \frac{z}{B} - p_5^* \frac{\dot{y}}{U} + \frac{2\pi^3}{V^{*2}} p_6^* \frac{y}{B} \end{pmatrix} \quad (3)$$

$$L_{se} = \frac{1}{2}\rho U^2 B \begin{pmatrix} -h_1^* \frac{\dot{z}}{U} - h_2^* \frac{B\dot{\theta}}{U} + h_3^* \theta + \dots \\ \frac{2\pi^3}{V^{*2}} h_4^* \frac{z}{B} - h_5^* \frac{\dot{y}}{U} + \frac{2\pi^3}{V^{*2}} h_6^* \frac{y}{B} \end{pmatrix} \quad (4)$$

$$M_{se} = \frac{1}{2}\rho U^2 B^2 \begin{pmatrix} -a_1^* \frac{\dot{z}}{U} - a_2^* \frac{B\dot{\theta}}{U} + a_3^* \theta + \dots \\ \frac{2\pi^3}{V^{*2}} a_4^* \frac{z}{B} - a_5^* \frac{\dot{y}}{U} + \frac{2\pi^3}{V^{*2}} a_6^* \frac{y}{B} \end{pmatrix} \quad (5)$$

In the aeroelastic forces per unit length defined above, h_i^* are the flutter derivatives for lift force; a_i^* are the flutter derivatives for the moment; p_i^* are the flutter derivatives for drag force; $V^* = U/(fB)$ is the reduced velocity, being *f* the vibration frequency.

For Step 1.2 the flutter derivatives coefficients are measured with dedicated imposed motion tests on the rigid sectional model of BB3. The eight flutter derivatives $(a_1^*, a_2^*, a_3^*, a_4^*, h_1^*, h_2^*, h_3^*, h_4^*)$ are measured considering five mean angles of attack: -4 deg, -2 deg, 0 deg, +2 deg, +4 deg. The flutter derivatives p_{1-6}^*, a_{5-6}^*, h_{5-6}^* are derived from quasi steady theory (QST) to complete the full set of flutter derivatives.

The buffeting forces F_{buff} per unit length due to incoming turbulent wind u and w are defined in frequency domain through the admittance functions:

$$\begin{Bmatrix} D_{buff} \\ L_{buff} \\ M_{buff} \end{Bmatrix} = \frac{1}{2}\rho U B \begin{bmatrix} \chi^*_{Du} & \chi^*_{Dw} \\ \chi^*_{Lu} & \chi^*_{Lw} \\ B\chi^*_{Mu} & B\chi^*_{Mw} \end{bmatrix} \begin{Bmatrix} U_u(f) \\ W_w(f) \end{Bmatrix} \quad (6)$$

Where $U_u(f)$ is the Fourier transform of $u(t)$ and $W_w(f)$ the Fourier transform of $w(t)$, positive upwards; χ^* are called admittance functions and they depend upon the reduced velocity *V** and the mean angle of attack. The χ^* are not measured in wind tunnel tests are defined using the quasi-steady values weighed by the Davenport function $A(V*)$ as:

$$\begin{aligned} \chi^*_{Du} &= 2C_D\, A(f^*) \\ \chi^*_{Lu} &= 2C_L\, A(f^*) \\ \chi^*_{Mu} &= 2C_M\, A(f^*) \\ \chi^*_{Dw} &= (K_D - C_L) A(f^*) \\ \chi^*_{Lw} &= (K_L + C_D) A(f^*) \\ \chi^*_{Mw} &= K_M\, A(f^*) \end{aligned} \quad (7)$$

where $A(V^*)$ is a real weighing function in reduced velocity:

$$A(V^*) = \frac{2}{(7/V^*)^2}\left(7/V^* - 1 + e^{-7/V^*}\right) \quad (8)$$

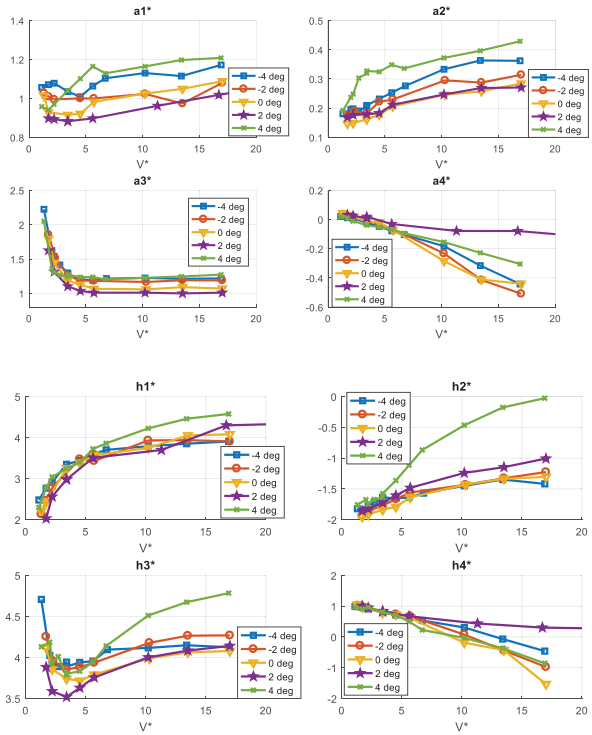

Figure 4. Flutter derivative coefficients

3.3 Required output for Step1.2 a/b

The following results are compared for both Cases a) and b):

1 Flutter stability:
   a. Critical flutter speed;

   b. frequencies and damping as a function of mean wind speed.
2 Buffeting response in turbulent flow:
   a. standard deviation of modal displacement as a function of mean wind speed;
   b. Comparison of power spectral densities (PSD) of midspan deck displacement as a function of mean wind speed.

4 Results of Step 1.2

Only a small selection of results is presented in this paper, while the full set of results will be presented at the conference and in a future work in the IABSE SEI journal.

The following results for Step 1.2a are shown in the following: flutter speeds, root mean square (RMS) trend of modal displacements as a function of wind speed, and PSDs of vertical and torsional displacements at midspan.

As explained in the previous publication [2], each contribution is defined anonymously by a number. To establish the reference result, the following procedure is applied:

1. The mean μ^* and the standard deviation σ^* of all data is computed.
2. The data outside $\mu^* \pm \sigma^*$ are considered outlier data.
3. The reference mean value μ and standard deviation σ are computed excluding the outlier data
4. Results within $\mu \pm \sigma$ are considered valid

4.1 Step1.2a – Flutter speed

Figure 5 shows ten different contributions for the assessment of the flutter speed of the considered. The reference is μ = 69.8 m/s and σ = 0.9 m/s.

4.2 Step1.2a – RMS displacements

Figure 6 shows six different contributions for the trend on modal RMS for the second vertical and first torsional mode (homologous modes). Results coming from both time domain (TD) and frequency domain (FD) methods are present. It is possible to notice that results are quite sparse. As an example, at 45 m/s, for the vertical mode is μ = 0.45 and σ = 0.03; for the torsional mode is μ = 8.2e-3 and σ = 1.3e-3.

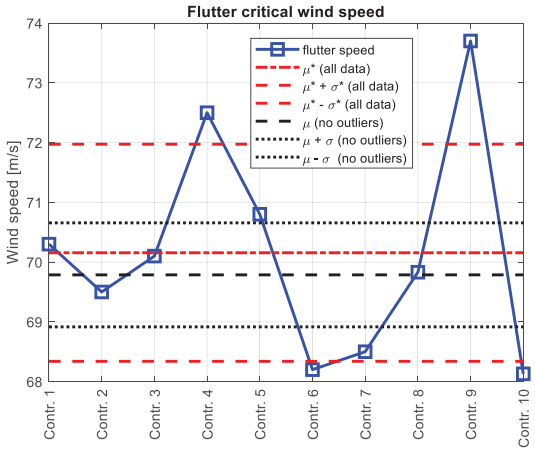

Figure 5. Step 1.2a Flutter critical wind speed results

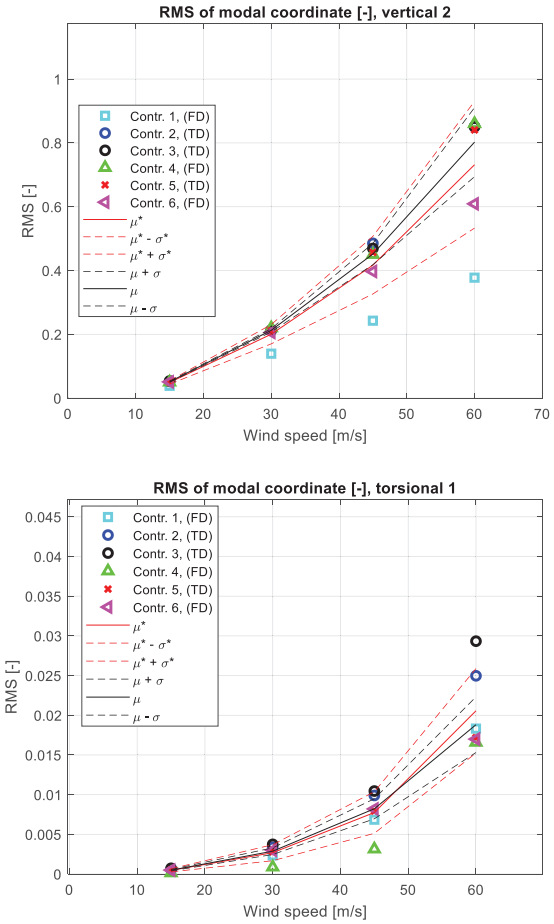

Figure 6. Step 1.2a RMS of the 2nd vertical and 1st torsional modes (homologous modes) as a function of wind speeds

4.3 Step1.2a – PSD of physical displacements at midspan

As another example of result, Figure 7 shows the PSD of the vertical displacement z and of the rotation $z_{eq} = \frac{B}{2}\theta$, of the midspan deck section at 45 m/s. Looking at the differences in the rotations it seems that the major difference is in the estimate of the resonant response. Looking at the vertical motion, it is clear that the first two contribution have a low frequency content missing in the others, and this would not have been notice looking only at the std values that are similar to the others.

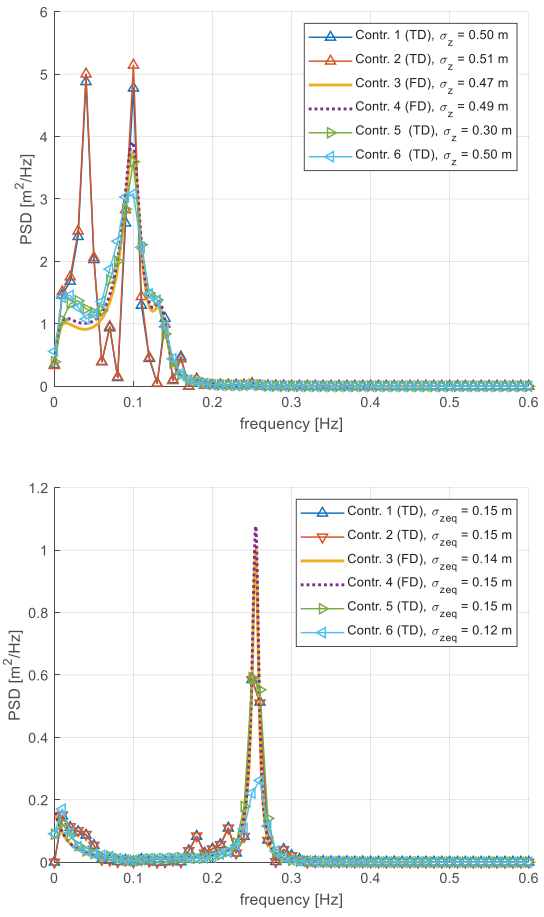

Figure 7. Step 1.2a RMS of the 1st vertical and 1st torsional modes as a function of wind speeds

5 Conclusions

This paper presents first results of Step 1.2 of the benchmark study: even for this rather simple problem, noticeable differences arose during the result comparisons.

Similar critical flutter velocities were predicted, however the trend of the RMS of the unstable modes as a function of the wind speed showed in some cases significant differences.

Buffeting response was computed in time and frequency domain, and it seems that the domain of simulation itself does not influence the dispersion of results, but it is the implementation of the computational models.

Removing the outliners and given the majority of the remaining predictions are reasonably close, the results within the interval $\mu \pm \sigma$ appear reasonable.

The comparison of results of case 1.2b will allow to investigate

6 References

[1] Diana G, Rocchi D, and Argentini T. Buffeting response of long span bridges: numerical-experimental validation of fluid-structure interaction models *IABSE Conference - Structural Engineering: Providing Solutions to Global Challenges,* 2015

[2] Aas-Jakobsen, K.; Allsop, A.; Kavrakov, I.; Larsen, A.; Øiseth, O.; Argentini, T.; Diana, G.; Omarini, S.; Rocchi, D.; Svendsen, M.; Larose, G.; Stoyanoff, S.; Kim, H.-K.; Hernandez; Wu, T.; Andersen, M. & Katsuchi, H. Super-long span bridge aerodynamics: First results of the numerical benchmark tests from task group 10 *IABSE Symposium, Nantes 2018: Tomorrow's Megastructures*, 2019, S34-71-S34-82

[3] Diana, G.; Rocchi, D.; Argentini, T. & Omarini, S. Flutter derivatives identification on a very large scale aeroelastic deck model *IABSE Conference, Vancouver 2017: Engineering the Future - Report*, 2017, 1997-2005

[4] Deodatis G. Simulation of ergodic multivariate stochastic processes. *Journal of Engineering Mechanics*. 1996; **122:**778-787.